NANOCAD Framework for Simulation of Quantum Effects in Nanoscale MOSFET Devices

Seonghoon Jin*, Chan Hyeong Park, In-Young Chung***, Young June Park*, and Hong Shick Min***

Abstract—**We introduce our in-house program, NANOCAD, for the modeling and simulation of carrier transport in nanoscale MOSFET devices including quantum-mechanical effects, which implements two kinds of modeling approaches: the top-down approach based on the macroscopic quantum correction model and the bottom-up approach based on the microscopic non-equilibrium Green's function formalism. We briefly review these two approaches and show their applications to the nanoscale bulk MOSFET device and silicon nanowire transistor, respectively.**

Index Terms—**MOSFET, quantum effect, density-gradient model, non-equilibrium Green's function (NEGF) formalism**

I. INTRODUCTION

As the MOSFET device shrinks aggressively toward the sub-10 nm regime, its various characteristic lengths are now comparable to the thermal de Broglie wavelength of electrons, and the emerging quantum mechanical effects strongly affect its electrical and optical characteristics. Nevertheless, the semi-classical transport models such as the drift-diffusion (DD) model [1] and the hydrodynamic (HD) model [2] have been widely used as the practical workhorse, especially in the industries, for the device design, characterization, and development of the compact model (CM). Therefore, the development strategy to provide the physical and numerical framework to compromise 'the physically accurate' and 'verifiable (so useful) in engineering application' is critically important in the design, analysis, and CM in the nanoscale era.

In this paper, we introduce a series of efforts based on our in-house program, NANOCAD, for modeling the MOSFET devices including the quantum effects. Hierarchically, there may be two approaches: top-down approach where the macroscopic drift-diffusion type equation is maintained and quantum correction is added to account for the quantum effects [3-15] and the bottom-up approach that starts from the more fundamental microscopic quantum transport formalism [16,17]. Certainly, there are pros and cons in each approach. The bottom-up approach based on the non-equilibrium Green's function (NEGF) or the Wigner distribution function [16-19] gives detailed physics associated with the wave nature of carriers, whereas it cannot be easily applied to rather complex multi-dimensional device structures. Also, there are discontinuities from the 'engineering models' that have been well tuned in the engineering fields. On the other hand, the top-down approach is the natural extension of the semi-classical transport model to include the quantum effects as a correction term [3-15]. In NANOCAD, we consider both approaches. For the top-down approach, we implement the density-gradient (DG) model that extends the DD or hydrodynamic (HD) model by including an effective quantum potential in the drift term. For the bottom-up approach, we implement the non-equilibrium Green's function formalism with phonon scattering mechanisms [20,21]. In Figure 1, the hierarchy of the quantum transport model in NANOCAD is depicted.

Manuscript received Jan. 13, 2006; revised Mar. 10, 2006.
* School of Electrical Engineering and Computer Science and Nano Systems Institute-NCRC, Seoul National University, Seoul 151-744, Korea
** Department of Electronics and Communications Engineering, Kwangwoon University, Seoul, Korea
*** Department of Electronic Engineering, Gyeongsang National University, Jinju, Korea
E-mail : sjin@isis.snu.ac.kr

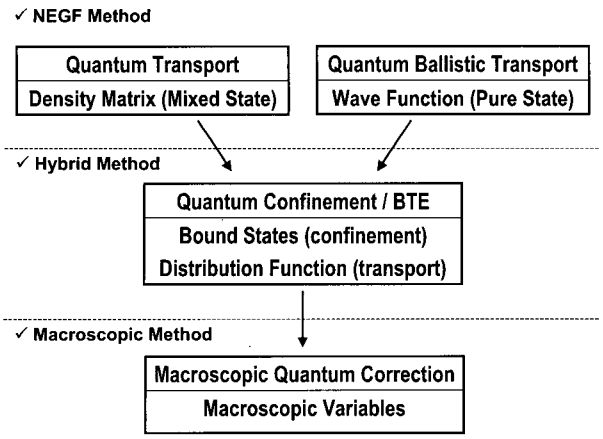

Fig. 1. Hierarchy of the quantum transport model in NANOCAD.

In Section II, we explain the density-gradient approach based on the hydrodynamic model, and show the simulation results of a 25-nm NMOSFET device. In Section III, we explain the bottom-up approach based on the NEGF method and show the simulation example applied to the silicon nanowire MOSFET where the cross section of the channel is the circle with diameter of 5 nm. We will conclude this paper by suggesting the future work in Section IV.

II. Density-Gradient Model

1. Basic Models

The density-gradient model can be derived from the Wigner distribution function defined as [18,19]

$$f(\mathbf{k},\mathbf{r},t)=\int_{-\infty}^{\infty} d\mathbf{u}\rho\left(\mathbf{r}+\frac{\mathbf{u}}{2},\mathbf{r}-\frac{\mathbf{u}}{2},t\right)e^{-i\mathbf{k}\cdot\mathbf{u}}, \tag{1}$$

where

$$\rho(\mathbf{r},\mathbf{r}')=\sum_i p_i\langle\mathbf{r}|i\rangle\langle i|\mathbf{r}'\rangle \tag{2}$$

is the density matrix and i labels a complete set of states and p_i are real-valued probabilities for the system to be in the i-th state. From the time evolution of the states, the equation of motion for the Wigner distribution function can be written as [18]

$$\frac{\partial f}{\partial t}+\mathbf{v}\cdot\nabla_r f-\sum_{l=0}^{\infty}\frac{(-1)^l(\nabla_r\cdot\nabla_k)^{2l+1}Vf}{\hbar 4^l(2l+1)!}=\left(\frac{\partial f}{\partial t}\right)_C \tag{3}$$

where $V = -q\psi$ denotes the spatially varying potential energy (ψ is the electrostatic potential). Macroscopic quantum hydrodynamic (QHD) equations can be derived from the moment expansion of (3). The expansion of the equation involves the integration of powers of moments (1, $\mathbf{k}$, k^2) against f to obtain conservation laws for the particle, momentum, and energy density. If we assume the steady-state, the isotropic and parabolic band structure, and that the collision term can be approximated by various relaxation times, the resulting conservation equations can be written as [7,15]

$$\sum_{i=1}^{3}\frac{\partial F_i}{\partial x_i}=0, \tag{4}$$

$$\sum_{j=1}^{3}\frac{\partial}{\partial x_j}\left(\frac{nk_BT_{qij}}{m^*}+\frac{F_iF_j}{n}\right)+\frac{n}{m^*}\frac{\partial V}{\partial x_i}=-\frac{F_i}{\tau_p}, \tag{5}$$

and

$$\sum_{i=1}^{3}\left(\frac{\partial S_i}{\partial x_i}+\frac{\partial V}{\partial x_i}F_i\right)+n\frac{w-w_0}{\tau_w}=0, \tag{6}$$

where m^* denotes the effective mass, n is the electron density, τ_p and τ_w are the momentum and the energy relaxation times,

$$F_i=n\hbar\langle k_i\rangle/m^* \tag{7}$$

is the i-th component of the carrier flux,

$$T_{qij}=\frac{\hbar^2}{m^*}\left\langle\left(k_i-\langle k_i\rangle\right)\left(k_j-\langle k_j\rangle\right)\right\rangle \tag{8}$$

is the temperature tensor,

$$w=\frac{\hbar^2\langle k^2\rangle}{2m^*} \tag{9}$$

is the average energy, w_0 is the average energy in equilibrium, and

$$S_i = \sum_{j=1}^{3}\left[Q_{ij} + F_i\left(\frac{k_B T_{qjj}}{2} + \frac{m^* F_j^2}{2n^2}\right) + F_j k_B T_{qij} \right] \tag{10}$$

is the energy flux density. In the above equation,

$$Q_{ij} = \frac{\hbar^3 n}{2m^{*2}}\left\langle \left(k_i - \langle k_i \rangle\right)\left(k_j - \langle k_j \rangle\right)^2 \right\rangle \tag{11}$$

is the heat flux. Note that the forms of (4), (5), and (6) are identical to those of the semi-classical counterparts. To simplify the above equations, we first neglect the drift energy in the energy flux and the convection term in the momentum balance equation. Note that these terms are also neglected in the conventional HD model. Secondly, we must approximate Q_{ij}, w-w_0, and T_{qij} in terms of the scalar electron temperature T. The heat flux is approximated by the Fourier law as

$$\sum_{j=1}^{3} Q_{ij} \approx -\kappa \frac{\partial T}{\partial x_i}, \tag{12}$$

where κ is the thermal conductivity. We can also assume that

$$w - w_0 \approx \frac{3}{2} k_B \left(T - T_0\right), \tag{13}$$

where T_0 is the lattice temperature. To approximate T_{qij}, we apply the temperature tensor expression and the relation between n and V valid at the thermal equilibrium as [15]

$$T_{qij} = T\delta_{ij} + \frac{\hbar^2}{12 m^* k_B^2 T}\frac{\partial^2 V}{\partial x_i \partial x_j} + O\left(\hbar^4\right), \tag{14}$$

$$V = -k_B T \ln\left(n/C\right) + O\left(\hbar^2\right), \tag{15}$$

and

$$\frac{\partial V}{\partial x_i} = -k_B T \frac{\partial \ln n}{\partial x_i} + O\left(\hbar^2\right) \tag{16}$$

to obtain final expressions up to $\hbar^2$ order. It is noted that $F_i T_{qjk} = F_i T \delta_{jk} + O(h^4)$ since F_i does not contain the zeroth order terms with respect to $\hbar^2$ by (15) and (16). The resulting equations for the carrier flux, energy balance, and energy flux can be written as

$$\mathbf{F} = \mu n \nabla\left(\psi + \psi_q\right) - \mu \nabla\left(\frac{k_B T}{q} n\right), \tag{17}$$

$$\nabla \cdot \mathbf{S} - q \nabla \psi \cdot \mathbf{F} + n \frac{3}{2} k_B \frac{T - T_0}{\tau_w} = 0, \tag{18}$$

and

$$\mathbf{S} = -\kappa \nabla T + \frac{5}{2} k_B T \mathbf{F}, \tag{19}$$

where $\mu = q\tau_p/m^*$ is the mobility and

$$\psi_q = 2b \frac{\nabla^2 \sqrt{n}}{\sqrt{n}} \tag{20}$$

is the effective quantum potential and $b = \hbar^2/(12qm^*)$ is the linear gradient coefficient. Note that the quantum correction only appears in the drift term of the carrier flux. The thermal conductivity can be written as

$$\kappa = \left(\frac{5}{2} + c\right)\frac{k_B^2}{q} T \mu n \tag{21}$$

using the Wiedemann-Frantz law.

We solve (4), (18), and (20) self-consistently with the Poisson equation

$$-\nabla \cdot \left(\varepsilon \nabla \psi\right) - q\left(p - n + N_D^+ - N_A^-\right) = 0, \tag{22}$$

where ε is the electric permittivity, p is the hole density, and N_D^+ and N_A^- are the ionized donor and acceptor densities. Note that our hydrodynamic density-gradient (HDG) model exactly reduces to the conventional HD model in the classical limit ($\psi_q \rightarrow 0$) and the DG model in thermal equilibrium ($T \rightarrow T_0$).

2. Simulation Results

We simulate a bulk NMOSFET whose effective channel length is 25 nm and physical oxide thickness is 1.5 nm [22]. The gate material is uniformly doped (5×10^{20} cm^{-3}) n^+ polysilicon and the channel doping profile is based on the super-halo to prevent the short-channel effect [23].

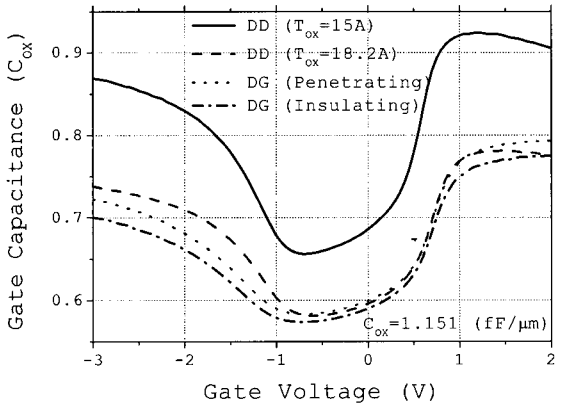

Fig. 2. Comparison of the CG-VG characteristics between the DD model tox=15 Å and tox=18.2 Å and the DG model (the penetrating boundary condition and the insulating boundary condition).

We first study the influence of the quantum effect on the gate capacitance. Figure 2 shows the C_G-V_G characteristics of the device. The quantum effect reduces the gate capacitance by 20% and increases the effective oxide thickness by 3.2 Å. The interface boundary condition also changes the gate capacitance. The penetrating boundary condition increases the gate capacitance slightly compared with the insulating boundary condition. To see the influence of the interface boundary condition, we plot the electron density in the inversion layer in Figure 3. As a reference, we calculate the electron density using the self-consistent Schrödinger equation solver. The electron density calculated from the penetrating boundary condition follows the Schrödinger equation solver very well, while the insulating boundary condition shifts the electron density away from the interface by about 1 Å. Figure 4 shows the electrostatic, quantum, and effective potentials along the 1D cut line through the center of the channel. The quantum potential smoothes the potential variation near the Si/SiO_2 interface, which prevents the electron density from varying discontinuously at the interface.

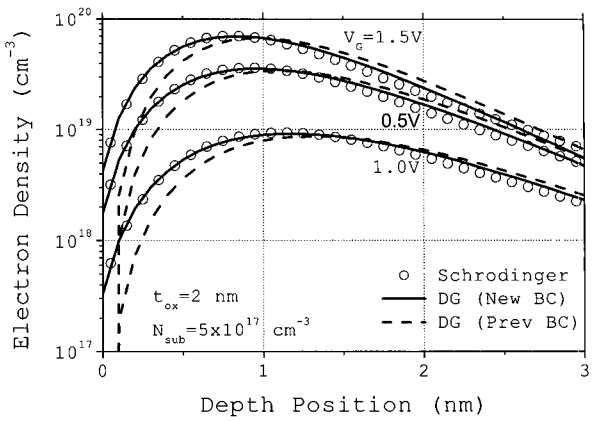

Fig. 3. Comparison of the electron density in the inversion layer between the Schrödinger equation solver, the HDG model with new boundary condition, and the HDG model with old boundary condition.

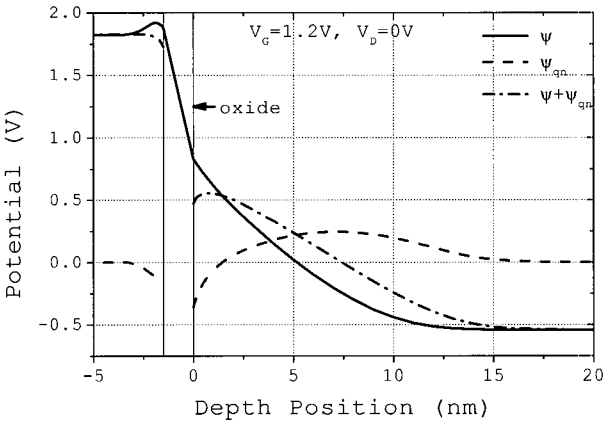

Fig. 4. Comparison of the electrostatic, quantum, and effective potentials along the 1D cut line through the center of the channel.

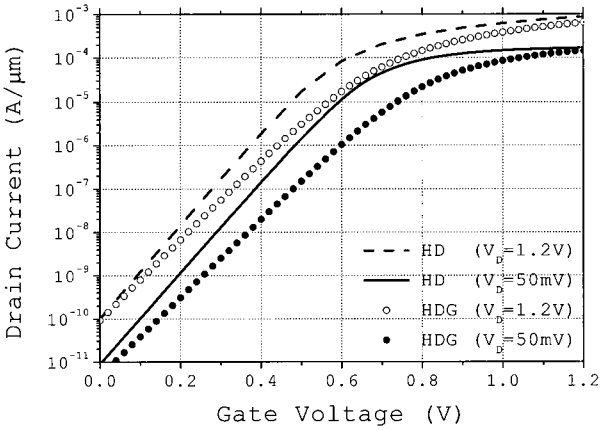

Fig. 5. Comparison of the ID-VG characteristics of the MOSFET between the HD and HDG models when VD is 50 mV and 1.2 V.

In Figure 5, we compare the I_D-V_G characteristics between the HD and HDG models. As we include the quantum effect, the subthreshold slope (SS) and drain-induced barrier lowering (DIBL) are increased from 93 mV/dec to 108 mV/dec and from 99 mV/V to 145 mV/V, respectively. Since the quantum confinement effect increases the effective oxide thickness, the gate electrode cannot control the channel charge effectively, which results in the degradation of the SS and DIBL.

Figure 6 shows the I_D-V_D characteristics calculated from the DG and HDG models. The HDG model predicts higher on-current up to 26%, which can be explained by the non-local transport effect.

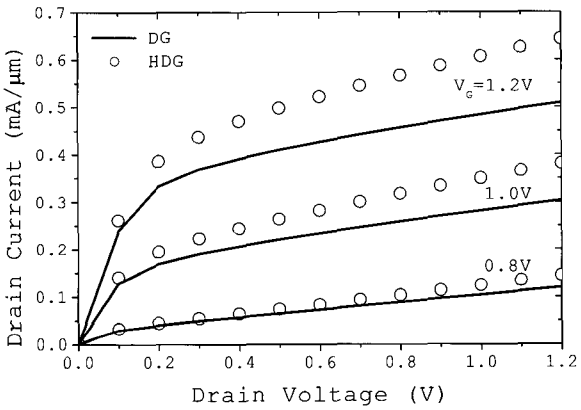

Fig. 6. Comparison of the ID-VD characteristics between the DG and HDG models when VG is 0.8, 1.0, and 1.2V.

III. NEGF Formalism With Phonon Scattering

1. Basic Models

In the NEGF formalism, the governing equations for the retarded (G^r), lesser ($G^<$), and greater ($G^>$) Green functions are as follows: [24]-[29]

$$\left[E-H(\mathbf{r}_1)\right]G^r(\mathbf{r}_1,\mathbf{r}_2;E) - \int d\mathbf{r}\,\Sigma^r(\mathbf{r}_1,\mathbf{r};E)G^r(\mathbf{r},\mathbf{r}_2;E)=\delta(\mathbf{r}_1-\mathbf{r}_2), \tag{23}$$

$$G^{>,<}(\mathbf{r}_1,\mathbf{r}_2;E)=\int d\mathbf{r}d\mathbf{r}'\,G^r(\mathbf{r}_1,\mathbf{r};E) \times\Sigma^{>,<}(\mathbf{r},\mathbf{r}';E)G^{r*}(\mathbf{r}_2,\mathbf{r}';E), \tag{24}$$

where H is the one-electron Hamiltonian and Σ^r, $\Sigma^>$, and $\Sigma^<$ are the retarded, greater, and lesser self-energy functions. For the intravalley and intervalley phonon scattering mechanisms, we can obtain spatially local self-energy functions from the deformation potential theory and the self-consistent Born approximation [20,21]. In this case, the quantum kinetic equations in the steady-state condition are simplified to [20, 21]

$$\left[E-H(\mathbf{r})+\frac{i\hbar}{2\tau(\mathbf{r};E)}\right]G^r(\mathbf{r},\mathbf{r}';E) =\delta(\mathbf{r}-\mathbf{r}'), \tag{25}$$

$$n(\mathbf{r};E)=\frac{2\hbar}{\pi}\int d\mathbf{r}'\frac{\left|G^r(\mathbf{r},\mathbf{r}';E)\right|^2}{\tau_p(\mathbf{r}';E)}, \tag{26}$$

$$p(\mathbf{r};E)=\frac{2\hbar}{\pi}\int d\mathbf{r}'\frac{\left|G^r(\mathbf{r},\mathbf{r}';E)\right|^2}{\tau_n(\mathbf{r}';E)}, \tag{27}$$

where $n(\mathbf{r};E)$ and $p(\mathbf{r};E)$ are the energy spectrum of the electron and hole densities and τ, τ_p, and τ_n are the time constants related to the phonon scattering mechanism [20], [21]. Derivation and discussion of (23)-(27) and the implementation details can be found in [20,21].

2. Simulation Results

We simulate cylindrical nanowire transistors as shown in Figure 7 with the channel lengths varying from 7 to 45 nm. In the simulation, we fix the lattice temperature to 300 K and consider five subbands per each valley, which gives 15 subbands in total. The bulk scattering parameters reported in [29] are used for the six kinds of intervalley phonon scattering mechanisms, whereas the scalar deformation potential constant Ξ for the intravalley phonon scattering mechanism is calibrated to 14.6 eV to reproduce the phonon-limited low field mobility in the MOS inversion layer [30]. The calculated low field mobility μ_0 in the channel of the nanowire from the NEGF formalism decreases from 670 to 614 $cm^2V^{-1}s^{-1}$ as the gate voltage V_G ramps up from –0.4 to 0.3 V, and we assume that μ_0 and the saturation velocity in the DD model are equal to 614 $cm^2V^{-1}s^{-1}$ and 1.07×10^7 cm/s, respectively.

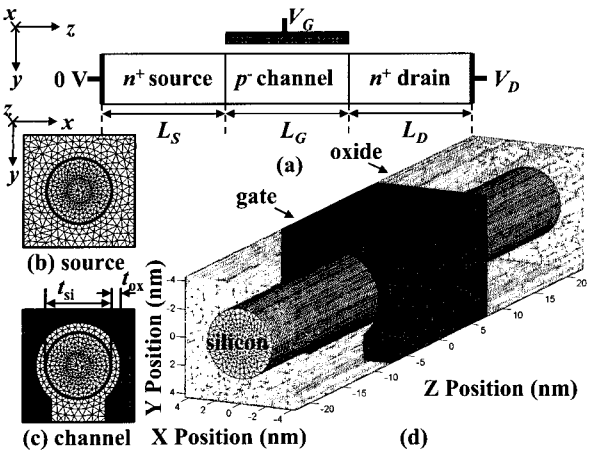

Fig. 7. Structure of the nanowire transistor (t_{si}=5 nm, t_{ox}=0.8 nm, L_S=15 nm, L_D=15 nm, and L_G=7 ~ 45 nm). Transport occurs along the z-direction and the spatial coordinate and the k-space coordinate are aligned. Ellipsoidal and parabolic energy band with three pairs of valley is considered.

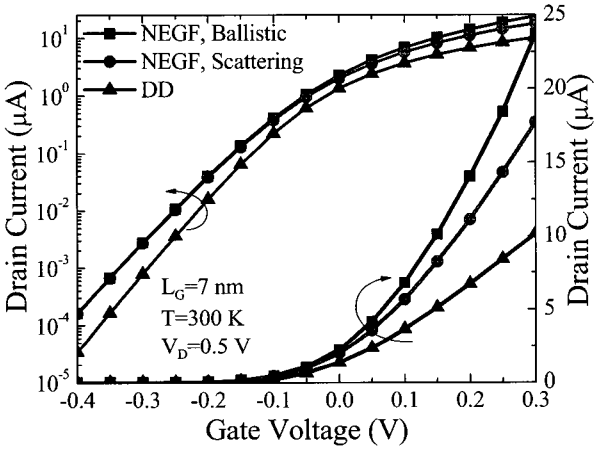

Fig. 8. Comparison of the I_D-V_G characteristics of the nanowire transistor with L_G=7 nm obtained from the NEGF formalism with and without the phonon scattering mechanisms and from the semi-classical DD model.

In Figure 8, we first compare I_D-V_G characteristics of the nanowire transistor with L_G=7 nm obtained from the DD model and the NEGF formalism with and without the electron-phonon interactions. Regardless of the phonon scattering, the NEGF formalism predicts larger subthreshold leakage current compared with the DD model due to the tunneling current from the source to drain, which is excluded in the DD model. The subthreshold currents obtained from the three different methods become very similar when L_G>10 nm because the tunneling probability decreases exponentially as the thickness of the barrier (channel length) increases. To compare the drain current in the above-threshold region, we compare on-currents (I_D when V_G=0.3 V and V_D=0.5 V) obtained from the three different models as well as their ratio (comparative magnitudes) as a function of the channel length in Figure 9. When the channel length is 7 nm, the on-current obtained from NEGF method with the phonon scattering is about 75 % of its ballistic limit, whereas the DD model predicts about 57 % of the NEGF method with the phonon scattering. Therefore, the electronic transport in the nanowire transistor with L_G=7 nm is close to its ballistic limit. As the channel length increases, however, the on-current obtained from the NEGF formalism in the presence of the phonon scattering gets closer to that from the DD model, whereas the overestimation of the drain current from the NEGF method in the ballistic limit gets larger. In Figure 10, we plot the average electron velocity and the electron density along the z-direction for L_G=45 nm.

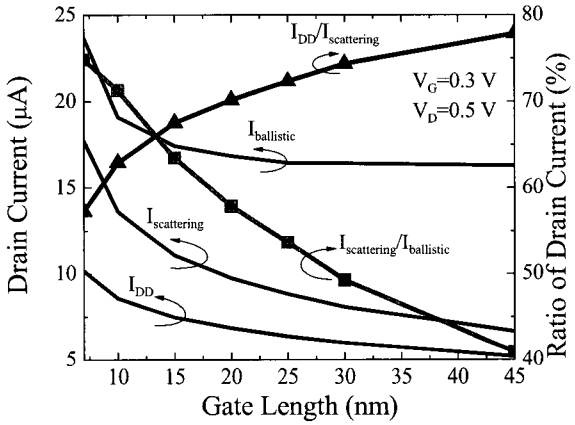

Fig. 9. Comparison of the on-currents (I_D when V_G=0.3 V and V_D=0.5 V) and their ratio as a function of the gate length calculated from the NEGF formalism with and without the phonon scattering mechanisms ($I_{scattering}$ and $I_{ballistic}$) and from the DD model (I_{DD}).

In the ballistic limit, the electron velocity and density do not change much from the entrance of the channel to the pinch-off region, whereas the electron velocity gradually increases and the electron density gradually decreases in the channel when the phonon scattering is present. In the DD model, the electron velocity is smallest and the electron density is largest in the channel. We also plot the energy spectrum of the electron density along the z-direction when L_G=7 and 45 nm in Figure 11. When L_G=7 nm, the electrons injected from the source to channel do not have enough time to interact with phonons before they exit the channel. Therefore, the average energy loss of electrons in the channel is not significant and the

electron transport can be regarded as quasi-ballistic. When L_G=45 nm, the electrons have more chance to interact with phonons, and the average energy loss of electrons in the channel is larger than that in the shorter channel device. Also, we can observe that the electric field in the channel before the pinch off region is relatively small, which suggests that the electron transport in this region can be treated macroscopically.

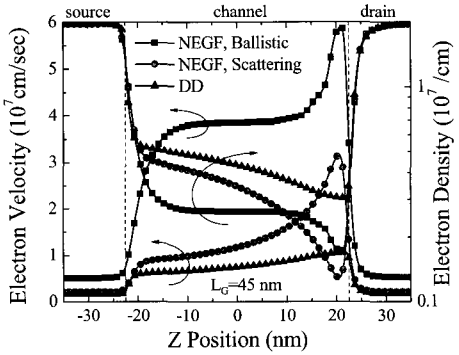

Fig. 10. Comparison of the average electron velocity and the electron density of the nanowire transistor with L_G=45 nm along the z-direction calculated from the NEGF formalism with and without the phonon scattering mechanisms and from the DD model.

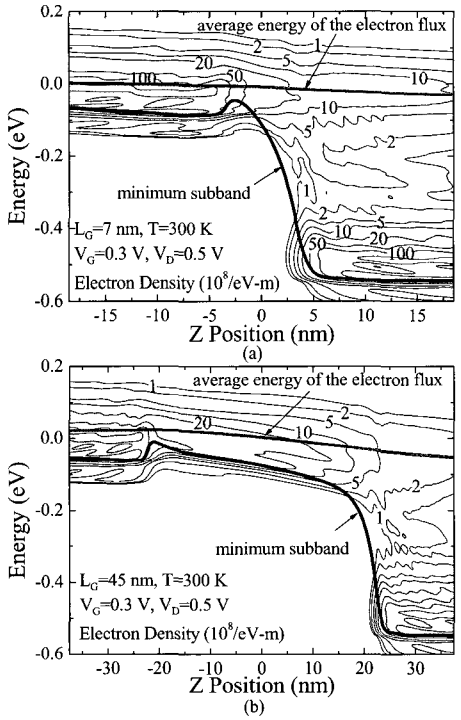

Fig. 11. Energy spectrum of the 1D electron density [in (10^8 $eV^{-1}m^{-1}$)] along the z-direction when the channel length is (a) 7 nm and (b) 45 nm obtained from the NEGF formalism with the phonon scattering mechanisms. The minimum subband energy level and the average energy of the electron flux are also plotted.

IV. Conclusions

We have explained the two approaches taken in NANOCAD to include the quantum effects in the semiconductor device simulations. First, we introduced the top-down approach, i.e. the extension of the classical drift-diffusion equation by the introduction of quantum correction terms. Secondly, the bottom-up approach based on the NEGF method was introduced. There, we have introduced our efforts to include the phonon scattering in the NEGF formalism.

Acknowledgments

This work was supported by the Brain Korea 21 project and the Nano-Systems Institute, National Core Research Center (NSI-NCRC) Program of KOSEF, Korea. C. H. Park's work was supported by Korea Research Foundation Grant funded by Korean Government (MOEHRD, Basic Research Promotion Fund) (KRF-2005-003-D00179) and present research has been conducted by the Research Grant of Kwangwoon University in 2004.

References

[1] S. Selberherr, *Analysis and Simulation of Semiconductor Devices*, Wien, Austria: Springer-Verlag, 1984.

[2] W. S. Choi, J. G. Ahn, Y. J. Park, H. S. Min, and C. G. Hwang, "A Time Dependent Hydrodynamic Device Simulator SNU-2D With New Discretization Scheme and Algorithm," *IEEE Trans. on CAD*, vol. 13, no. 7, pp. 899-908, July 1994.

[3] M. G. Ancona and H. F. Tiersten, "Macroscopic physics of the silicon inversion layer," *Phys. Rev. B*, vol. 35, no. 15, pp. 7959-7965, May 1987.

[4] M. G. Ancona and G. J. Iafrate, "Quantum correction to the equation of state of an electron gas in a semiconductor," *Phys. Rev. B*, vol. 39, no. 13, pp. 9536-9540, May 1989.

[5] J.-R. Zhou and D. K. Ferry, "Simulation of Ultra-Small GaAs MESFET Using Quantum Moment Equations," *IEEE Trans. on ED*, vol. 39, no. 3, pp.

473-478, March 1992.

[6] H. L. Grubin, T. R. Govindan, and J. P. Kreskovsky, "Transport via the Liouville equation and moments of quantum distribution functions," *Solid-State Electronics*, vol. 36, no. 12, pp. 1697-1709, 1993

[7] C. L. Gardner, "The Quantum Hydrodynamic Model for Semiconductor Devices," *SIAM Journal on Applied Mathematics*, vol. 54, no. 2, pp. 409-427, April 1994.

[8] D. K. Ferry, R. Akis, and D. Vasileska, "Quantum Effects in MOSFETs: Use of an Effective Potential in 3D Monte Carlo Simulation of Ultra-Short Channel Devices," *Proc. of IEDM*, pp. 287-290, December 2000.

[9] M. G. Ancona, Z. Yu, R. W. Dutton, P. J. V. Voorde, M. Cao, and D. Vook, "Density-gradient analysis of MOS tunneling," *IEEE Trans. on ED*, vol. 47, no. 12, pp. 2310-2319, December 2000.

[10] Z. Yu, R. W. Dutton, and D. W. Yergeau, "Macroscopic quantum carrier transport modeling," *Proc. of SISPAD*, pp. 1-9, September 2001.

[11] D. Connelly, Z. Yu, and D. W. Yergeau, "Macroscopic Simulation of Quantum Mechanical Effects in 2-D MOS Devices via the Density Gradient Method," *IEEE Trans. on ED*, vol. 49, no. 4, pp. 619-626, April 2002.

[12] E. Lyumkis, R. Mickevicius, O. Penzin, B. Polsky, K. El Sayed, A. Wettstein, and W. Fichtner, "Simulation of Ultrathin, Ultrashort Double-Gated MOSFETs with the Density Gradient Transport Model," *Proc. of SISPAD*, pp. 271-274, September 2002.

[13] J. R. Watling, A. R. Brown, A. Asenov, A. Svizhenko, and M. P. Anantram, "Simulation of direct source-to-drain tunneling using the density gradient formalism: Non-equilibrium Green's function calibration," *Proc. of SISPAD*, pp. 267-270, September 2002.

[14] S. Jin, Y. J. Park, and H. S. Min, "A Numerically Efficient Method for the Hydrodynamic Density-Gradient Model," *Proc. of SISPAD*, pp. 263-266, September 2003.

[15] S. Jin, Y. J. Park, and H. S. Min, "Simulation of Quantum Effects in the Nano-scale Semiconductor Device," *Journal of Semiconductor Technology and Science*, vol. 4, no. 1, March 2004.

[16] L. P. Keldysh, "Diagram technique for nonequilibrium process," *Sov. Phys. JETP*, vol. 20, no. 4, pp. 1018-1026, Apr. 1965.

[17] L. P. Kadanoff and G. Baym, *Quantum Statistical Mechanics*. New York: Benjamin, 1962.

[18] W. R. Frensley, "Boundary conditions for open quantum systems driven far from equilibrium," *Rev. Mod. Phys.*, vol. 62, no. 3, pp. 745-791, July 1990.

[19] E. Wigner, "On the Quantum Correction For Thermodynamic Equilibrium," *Phys. Rev.*, vol. 40, pp. 749-759, June 1932.

[20] S. Jin, Y. J. Park, and H. S. Min, "A three-dimensional simulation of quantum transport in silicon nanowire transistor in the presence of electron-phonon interactions," submitted to Journal of Applied Physics, 2006.

[21] S. Jin, "Modeling of Quantum Transport in Nano-Scale MOSFET Devices," Ph.D. dissertation, Seoul National University, Feb. 2006.

[22] D. A. Antoniadis, I. J. Djomehri, K. M. Jackson, and S. Miller, *Well-Tempered Bulk-Si NMOSFET Device Home Page*, http://www-mtl.mit.edu/Well/, Microsystems Technology Laboratory, MIT.

[23] Y. Taur, C. H. Wann, and D. J. Frank, "25 nm CMOS Design Considerations," *Proc. of IEDM*, pp. 789-792, December 1998.

[24] J. Rammer, "Quantum field-theoretical methods in transport theory of metals," *Rev. Mod. Phys.*, vol. 58, no. 2, pp. 323-359, Apr. 1986.

[25] G. D. Mahan, "Quantum Transport Equation for Electric and Magnetic Fields," *Physics Reports*, vol. 145, no. 5, pp. 251-318, 1987.

[26] S. Datta, *Electronic Transport In Mesoscopic Systems*. New York: Cambridge University Press, 1995.

[27] H. Haug and A.-P. Jauho, *Quantum Kinetics in Transport and Optics of Semiconductors*, Springer series in solid-state sciences. Springer, 1996.

[28] S. Datta, *Quantum Transport: Atom to Transistor*. Cambridge University Press, 2005.

[29] C. Jacoboni and L. Reggiani, "The Monte Carlo method for the solution of charge transport in semiconductors with applications to covalent materials," *Rev. Mod. Phys.*, vol. 55, no. 3, pp. 645-705, July 1983.

[30] D. Esseni, A. Abramo, L. Selmi, and E. Sangiorgi, "Physically Based Modeling of Low Field Electron Mobility in Ultrathin Single- and Double-Gate SOI n-MOSFETs," *IEEE Trans. Electron Devices*, vol. 50, no. 12, pp. 2445-2455, Dec. 2003.

Seonghoon Jin was born in Korea, in 1978. He received the B.S. and Ph.D. degrees in electrical engineering from Seoul National University, Seoul, Korea, in 2001 and 2006, respectively. Currently, he is a Post-Doctoral Researcher with the Nano Systems Institute, Seoul National University. His current research interests include quantum transport modeling in the nano-scale MOSFET devices, device reliability and fluctuation modeling of DRAM and FLASH memory devices, noise modeling in semiconductor devices, and developing a comprehensive three-dimensional simulation program for semiconductor devices.

Chan Hyeong Park received the B.S., M.S., and Ph.D. degrees in electronics engineering from Seoul National University in 1992, 1994, and 2000, respectively. From 2000 to 2003, he was a Visiting Scientist of Research Laboratory of Electronics at Massachusetts Institute of Technology, U.S.A. He joined the faculty of Kwangwoon University, Korea in 2003, where he is currently an Assistant Professor in the Department of Electronics and Communications Engine. ering. His current research interests are the modeling and simulation of noise processes in CMOS radio-frequency integrated circuits (RFICs) and carrier transport in nanoscale devices.

In-Young Chung received the B.S. and M.S. and Ph. D. degrees in electronics engineering from Seoul National University, Seoul, Korea, in 1994, 1996 and 2000 respectively. In 2000, he joined Samsung Electronics Co. LTD where he had been involved in the design of high-speed DRAM interfaces. In 2004, he joined the faculty of the Department of Electronic Engineering, Gyeongsang National University. His research interests include low-power circuit design, high-speed interfaces, and nano-device technologies.

Young June Park received the B.S. and M.S. degrees from Seoul National University, Seoul, Korea in 1975 and 1977, respectively, and the Ph.D. degree from the University of Massachusetts, Amherst, in 1983.

From 1983 to 1985, he worked for the Device Physics and Technology Department, IBM, East Fishkill, NY. In 1985, he joined Gold Star Semiconductor Company, Anyang, Kyungki, (currently Hynix Semi-conductor Inc.) to work in the area of the CMOS technology. Since 1988, he has been with Seoul National University (SNU), where he is a Professor in the School of Electrical Engineering and Computer Science. In 1993, he spent his sabbatical year at Stanford University, Stanford, CA, and performed research on advance semiconductor transport model. From 1996 to 2001, he served the Inter-University Semiconductor Research Center (ISRC), SNU, as a Director. In 2001, he was on a leave of absence to work for Hynix Semiconductor Inc. as a Director of the Memory Research and Development Division. His areas of interest are the advanced device structures, device/noise and reliability modeling, and low-power circuit technology. Since 2003, he serves the director of the Nano System Institute under the NCRC (Nano Core Research Center) program supported by KOSEF, Korea. His current area of interest is the Nano MOSFET modeling and MOSFET applications to Bio-systems.

Hong Shick Min received the B.S. degree in electronics engineering from Seoul National University, Seoul, Korea, in 1966, and M.S. and the Ph.D. degrees in electrical engineering from the University of Minnesota, Minneapolis, in 1969 and 1971, respectively.

From 1971 to 1972, he was a Postdoctoral Fellow at the University of Minnesota. In 1973, he joined the Department of Electronics Engineering at Korea University, Seoul, as an Assistant Professor. Since 1976, he has been with the School of Electrical Engineering, Seoul National University, where he is currently a Professor. His main research interests include noise in semiconductors and semiconductor devices.